ELSEVIER

Ceramics International 31 (2005) 11–14

CERAMICS INTERNATIONAL

www.elsevier.com/locate/ceramint

Phase transformations of Li_2O–Al_2O_3–SiO_2 glasses with CeO_2 addition

A.M. Hu*, K.M. Liang, F. Zhou, G.L. Wang, F. Peng

Department of Materials Science and Engineering, Tsinghua University, Beijing 100084, PR China

Received 10 September 2003; received in revised form 5 November 2003; accepted 21 January 2004

Abstract

The nucleation and crystallization behavior of Li_2O–Al_2O_3–SiO_2 glasses with addition of 5 wt.% CeO_2 were investigated. With CeO_2 addition, the glass transition temperature (T_g) and the crystallization peak temperature (T_p) decreased. The transformations of glass to β-quartz and of β-quartz to β-spodumene were accelerated by addition of CeO_2. The values of crystallization activation energy (E) and Avrami exponent (n) determined by the Kissinger equations and the Augis–Bennett equation were 282 ± 7 kJ/mol and 3.2 ± 0.2, respectively, while without addition of CeO_2, the values were 323 ± 7 kJ/mol and 2.8 ± 0.2. The results suggest that addition of 5 wt.% CeO_2 serving as a flux also promotes crystallization.

Keywords: D. Glass; D. Glass-ceramics; Nucleation; Crystallization

1. Introduction

Lithium aluminum silicate (LAS) glass-ceramics have low thermal expansion coefficient as well as excellent thermal and chemical durability [1–6], and have achieved great industrial and economic importance. However, LAS glasses have high melting temperatures and high viscosity making them difficulty to produce, so addition of fluxes such as B_2O_3, PbO, alkali oxides, and alkali earth oxides had been used in LAS glass ceramics to lower the melting temperature for many years [7–14]. But these additions cause problems of high thermal expansion coefficient and/or loss of transparency. Lanthanon metal oxides, Y_2O_3 and La_2O_3, have been added in LAS glass ceramics; with 8 wt.% Y_2O_3 and La_2O_3 addition the transformation temperature of β-quartz to β-spodumene was increased from about 900 °C to above 1000 °C, but upon addition of Y_2O_3 and La_2O_3, the melting temperatures of the glass systems were high, above 1650 °C [15]. Sohn et al. [16] found that CeO_2 as a flux markedly decreased viscosity in MgO–Al_2O_3–SiO_2 glasses, and had a little influence on thermal expansion, mechanical properties and chemical durability of glasses. Holand et al. [17] found that CeO_2 could serve as nucleating agents in K_2O–Al_2O_3–SiO_2 glasses and caused the crystallization mechanism to change from surface to volume crystallization. However, there are few reports about LAS glass ceramics with CeO_2 additions.

In this study, we prepare LAS glass ceramics by adding CeO_2 as flux and observe the effects of CeO_2 addition on the crystallization and nucleation.

2. Experimental procedures

The initial materials were analytical grade reagents SiO_2, Al_2O_3, Li_2CO_3, MgO, ZnO, P_2O_5, TiO_2, ZrO_2, and CeO_2. The detailed compositions of these glasses were given in Table 1. P_2O_5 with an equivalent amount of Al_2O_3, were chosen as the main components to decrease the melt viscosity, then enter the structure of β-quartz [1]. A stuffed β-quartz structure in the form of $AlPO_4$ quartz-like groupings, should result in a more loose crystalline structure [18–20] that should lead to an increase in the concentration of cerium ions entering the crystalline phase. The initial bubble free glasses were melted in an electric furnace for 5 h at temperatures of 1540 and 1570 °C for glass with and without CeO_2 addition, then poured onto a metal plate and annealed at 600 °C.

Differential thermal analysis (DTA) of annealed glass specimens was done using a Dupont 2100 Thermal Analyzer. After crushing annealed glasses to about 100–200 μm, non-isothermal experiments were performed by heating

---

* Corresponding author. Tel.: +86-10-62773392.
E-mail address: huanmin@mails.tsinghua.edu.cn (A.M. Hu).

0272-8842/\$30.00 © 2004 Elsevier Ltd and Techna S.r.l. All rights reserved.
doi:10.1016/j.ceramint.2004.01.012

Table 1
Composition of glasses (wt.%)

Sample no.	Li_2O	Al_2O_3	SiO_2	MgO	ZnO	TiO_2	ZrO_2	P_2O_5	CeO_2
1	4.0	25.0	57.0	1.0	1.0	2.0	2.0	8.0	0
4	3.8	23.8	54.2	0.9	0.9	1.9	1.9	7.6	5.0

Table 2
The values of T_p (K) at different heating rates

Sample no.	$\alpha = 5$ K/min	$\alpha = 10$ K/min	$\alpha = 15$ K/min	$\alpha = 20$ K/min
1	1118 ± 2	1136 ± 2	1153 ± 2	1165 ± 2
2	1020 ± 2	1046 ± 2	1063 ± 2	1072 ± 2

30 mg samples in a Pt crucible with Al_2O_3 as the reference material in the temperature range between 20 and 1200 °C at heating rates of 5–20 °C/min.

X-ray diffraction (XRD) investigations were done with a D-max-RB diffractometer with Cu Kα radiation in the 2θ range from 10 to 70° at 0.02° steps.

Scanning electron microscopy (SEM) was done with a JSM-6301F. Energy dispersion X-ray spectroscopy, EDS, was used to identify the chemical composition of the glass and the crystalline phases. Optical mount specimens were prepared by standard metallographic techniques using chemical etching in an HF solution (5%) for 1.5 min. Etched glass-ceramic samples were coated with a thin layer of gold.

3. Results and discussion

DTA curves for the two glass samples at a heating rate of 10 K/min are shown in Fig. 1. Only one exotherm was observed in each curve, the same as in previous investigations [1–5], which are associate with precipitation of a stuffed β-quartz solid solution. According to Fig. 1, the glass transition temperatures (T_g) decreased from 725 to 674 °C and the glass crystallization peak temperatures (T_p) shifted from 872 to 851 °C with CeO_2 addition; addition of CeO_2 not only lowers the viscosity of the glass, but also promotes crystallization [21].

The characteristics of crystal growth in glass can be investigated using the Johnson–Mehl–Avrami (JMA) equation [22,23]:

$$-\ln(1 - x) = (kt)^n \tag{1}$$

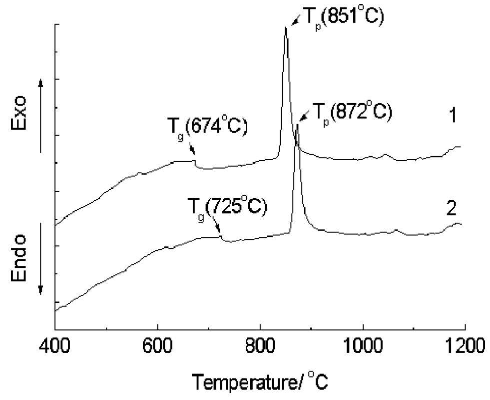

Fig. 1. DTA curves of glass samples ($\alpha = 10$ K/min): (1) with CeO_2; (2) without CeO_2 addition.

where x is the volume fraction of crystallized phase at time t; n, Avrami exponent related to the mechanism of crystallization; and k, effective reaction rate, related to the absolute temperature, T, by an Arrhenius type equation:

$$k = \nu \exp\left(-\frac{E}{RT}\right) \tag{2}$$

where ν is the frequency factor; R, gas constant; and E, activation energy of crystal growth. From Eqs. (1) and (2), non-isothermal crystallization kinetics of glass can be described by the expression [24]:

$$\ln\frac{T_p^2}{\alpha} = \frac{E}{RT_p} + \ln\frac{E}{R\nu} \tag{3}$$

where T_p is the crystallization peak maximum temperature in a DTA curve and α is the heating rate of DTA. The crystallization exothermal peak maximum temperatures at different heating rates are given in Table 2, as listed in Table 2. T_p decreases at each heating rate from no. 1 to no. 4. The plot of $\ln(T_p^2/\alpha)$ versus $1/T_p$ is expected to be linear which is shown in Fig. 2, and values of E and ν can be derived from the slope and intercept. Values of E and frequency factor ν change from 323 ± 7 kJ/mol, $(3.4 \pm 0.2) \times 10^{12}\ \mathrm{min}^{-1}$ to 282 ± 7 kJ/mol, $(4.1 \pm 0.3) \times 10^{13}\ \mathrm{min}^{-1}$ as doped with 5 wt.% CeO_2. Addition of CeO_2, decreases the viscosity of the glass matrix [16], which favors diffusion, so the frequency factor ν increases. The activation energy for crystal growth, correlating with the energy barrier of transition from glass to crystal, also decreases. The low energy barrier and high diffusion velocity lead to more rapid crystallization of the glass [22].

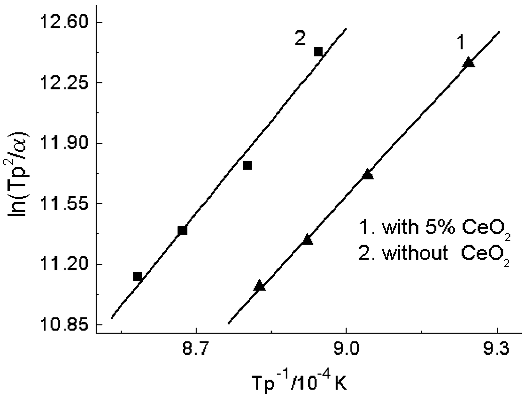

Fig. 2. The plots of $\ln(T_p^2/\alpha)$ vs. $1/T_p$ for the glasses.

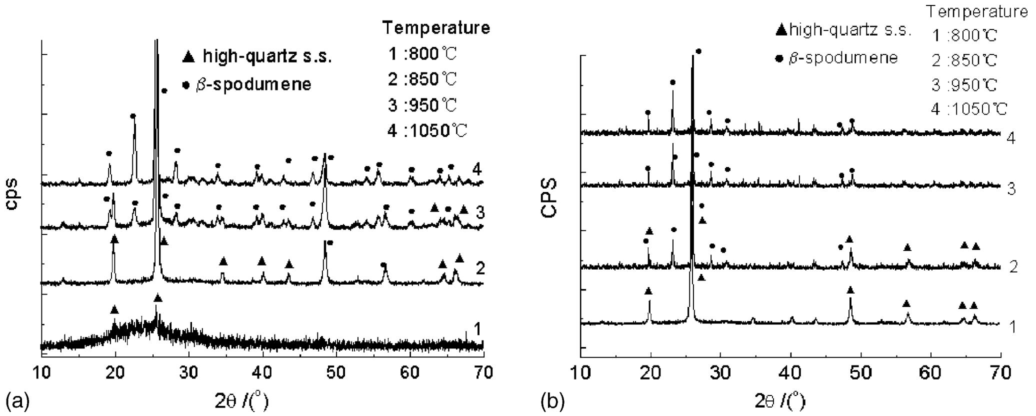

Fig. 3. XRD patterns of the crystallization glasses heated at 800, 850, 950, and 1050 °C for 1 h: (a) without CeO_2; (b) with 5 wt.% CeO_2.

With the values of activation energy, the Avrami parameter (n) was calculated using the Augis–Bennett equation [25]:

$$n = \frac{2.5}{\Delta T}\frac{RT_p^2}{E} \tag{4}$$

where ΔT is the full width of the exothermic peak at the half maximum intensity. Values of n close to 1 imply that surface crystallization dominates overall crystallization, values of n close to 2 imply that two-dimension crystallization, values of 3 imply bulk crystallization and values of 4 indicate homogeneous crystallization. By addition of CeO_2, the n value increases from 2.8 ± 0.2 to 3.3 ± 0.2. This indicates that the crystallization mechanism changes from bulk crystallization to homogeneous crystallization.

Fig. 3a and b show the powder XRD patterns of glasses doped with and without CeO_2 addition after being heated at the optimum nucleation temperatures: 730 and 760 °C, respectively, for 2 h, then heated at 800, 850, 900, and 1050 °C for 1 h. The samples without CeO_2 addition, after 800 °C for 1 h, show a broad scattering spectrum and small amounts of high-quartz s.s. formed in the glass. For the glass samples heated at higher temperature, 850 °C, the intensity of

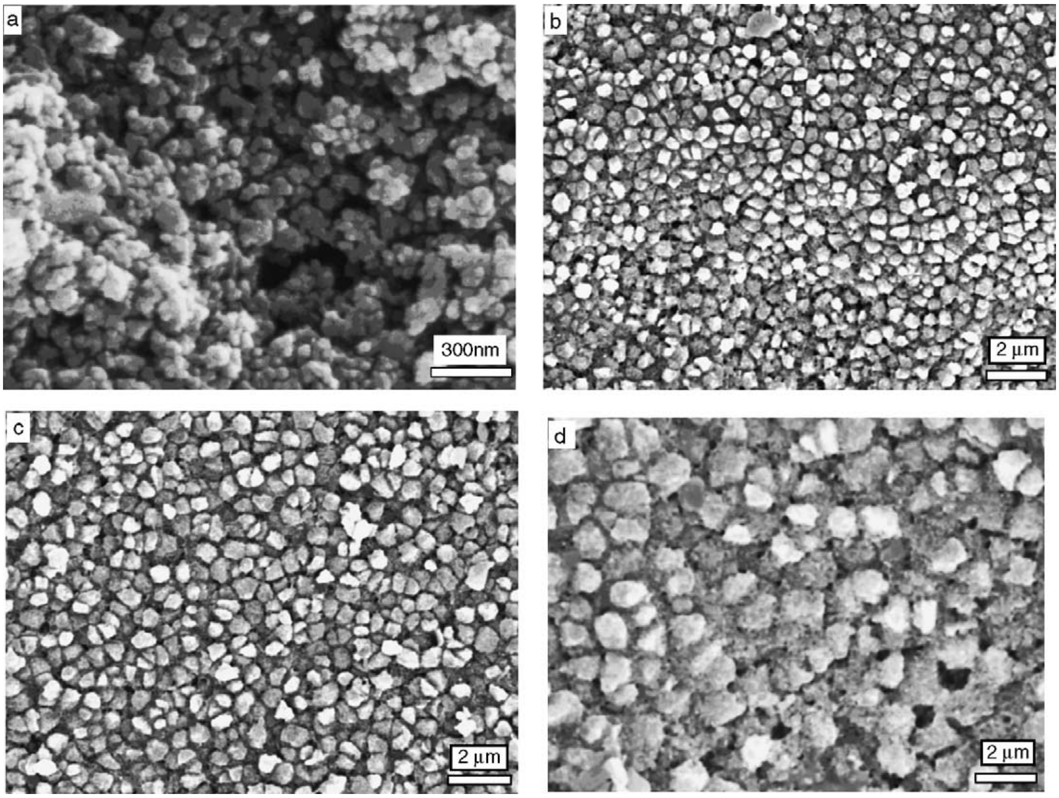

Fig. 4. SEM pictures showing the microstructure of the crystallized glass samples with 5 wt.% CeO_2 addition heated at: (a) 800 °C; (b) 850 °C; (c) 950 °C, and (d) 1050 °C for 2 h.

high-quartz s.s. increase and the broad scattering spectrum disappeared; this indicates the near completion of the crystallization process. β-Spodumene appeared and high-quartz s.s. decreased after being heated at 950 °C. β-Spodumene increased and high-quartz s.s. disappeared at 1050 °C. Samples with 5 wt.% CeO_2 addition gave large amounts of β-quartz s.s. after being heated at 800 °C for 1 h; as the heating temperature increased to 850 °C, the peak of β-spodumene grew at the expense of the high-quartz s.s.; at 950 °C, β-quartz s.s. disappeared and only β-spodumene was identified. It can be concluded that β-quartz s.s. precipitated directly from the glass, then transformed to β-spodumene either with or without CeO_2 addition. The transformations of glass to β-quartz s.s. and β-quartz s.s. to β-spodumene were all accelerated by addition of CeO_2.

Fig. 4a–d show the microstructure of the crystallized glass samples with 5 wt.% CeO_2 addition heated at 800, 850, 950, and 1050 °C for 1 h, respectively. After being heated at 800 °C, 2 h, the grain size is about 100 nm, according to XRD analysis; the sample is mainly stuffed high-quartz s.s. The mean crystal size increased with increasing crystallization temperature. EDS analysis showed that cerium initially present in the parent glass could be incorporated in the high-quartz s.s. and β-spodumene.

4. Conclusions

With 5 wt.% CeO_2 addition, β-quartz solid solution initially precipitates from the glass, then transforms to β-spodumene at higher temperature; the transformations of glass to β-quartz s.s. and β-quartz s.s. to β-spodumene were all accelerated by CeO_2. The values of crystallization activation energy (*E*) and Avrami exponent (*n*) were 282 ± 7 kJ/mol and 3.2 ± 0.2, while without addition of CeO_2, the values were 323 ± 7 kJ/mol and 2.8 ± 0.2. The results suggest that addition of 5 wt.% CeO_2 serving as a flux also promotes crystallization.

References

[1] G.H. Beall, L.R. Pinckney, Nanophase glass-ceramics, J. Am. Ceram. Soc. 82 (1999) 5–16.

[2] L. Arnault, M. Gerland, A. Riviere, Microstructural study of two LAS-type glass-ceramics and their parent glass, J. Mater. Sci. 35 (2000) 2331–2345.

[3] P. Riello, P. Canto, N. Comelato, et al., Nucleation and crystallization behavior of glass-ceramic materials in the Li_2O–Al_2O_3–SiO_2 system of interest for their transparency properties, J. Non-Cryst. Solids 288 (2001) 127–133.

[4] L. Barbieri, C. Leonelli, T. Manfredini, et al., Nucleation and crystallization of a lithium aluminosilicate glass, J. Am. Ceram. Soc. 80 (1997) 3077–3083.

[5] J.Y. Hsu, R.F. Speyer, Influences of zirconia and silicon nucleating agents on the devitrification of $Li_2O{\cdot}Al_2O_3{\cdot}6SiO_2$ glasses, J. Am. Ceram. Soc. 73 (1990) 3585–3593.

[6] V. Maier, G. Mueller, Mechanism of oxide nucleation in lithium aluminosilicate glass-ceramics, J. Am. Ceram. Soc. 70 (1987) C176–C178.

[7] M.C. Wang, M.H. Hon, F.S. Yen, Growth behavior and morphology of lithium–calcium aluminosilicate (LCAS) glasses, J. Cryst. Growth 91 (1988) 155–162.

[8] M.C. Wang, M.H. Hon, Effect of CaO addition on crystallization processes of Li_2O–Al_2O_3–SiO_2–TiO_2 glasses, J. Ceram. Soc. Jpn. 100 (1992) 1285–1291.

[9] C. Leonelli, T. Manfredini, M. Paganelli, et al., Li_2O–Al_2O_3–SiO_2–$Me^{II}O$ glass-ceramic systems for tile glaze application, J. Am. Ceram. Soc. 74 (1991) 983–987.

[10] L. Barbieri, A.B. Corradi, C. Leonelli, et al., Effect of TiO_2 addition on the properties of complex aluminosilicate glasses and glass-ceramics, Mater. Res. Bull. 32 (1997) 637–648.

[11] J.M. Rincon, M. Romero, J. Marco, V. Caballer, Some aspect of crystallization microstructure on new glass-ceramic glazes, Mater. Res. Bull. 33 (1998) 1159–1164.

[12] A.W.A. Elshennawi, E.M.A. Hamzawy, G.A. Khater, A.A. Omar, Crystallization of some aluminosilicate glasses, Ceram. Int. 27 (2001) 725–730.

[13] J.J. Shyu, M.T. Chiang, Sintering and phase transformation in B_2O_3/P_2O_5-doped $Li_2O{\cdot}Al_2O_3{\cdot}4SiO_2$ glass-ceramics, J. Am. Ceram. Soc. 83 (2000) 635–639.

[14] K. Davkova, S. Zafirovski, S. Pocev, V. Zlatanovic, Preparation of precipitated batch composition for glass ceramics in the system SiO_2–Al_2O_3–Li_2O–TiO_2–B_2O_3–ZnO–MgO, Glass Technol. 41 (2000) 197–198.

[15] J.J. Shyu, C.S. Hwang, Effects of Y_2O_3 and La_2O_3 addition on the crystallization of $Li_2O{\cdot}Al_2O_3{\cdot}4SiO_2$ glass-ceramic, J. Mater. Sci. 31 (1996) 2631–2639.

[16] S.B. Sohn, S.Y. Choi, Y.K. Lee, Controlled crystallization and characterization of cordierite glass-ceramics for magnetic memory disk substrate, J. Mater. Sci. 35 (2000) 4815–4821.

[17] W. Holand, M. Frank, V. Rheinberger, Surface crystallization of leucite in glasses, J. Non-Cryst. Solids 180 (1995) 292.

[18] T.I. Chuvaeva, I.P. Alekseeva, E.V. Podushko, A study of b-quartz solid solutions in the SiO_2–Al_2O_3–P_2O_5–Li_2O system, Zh. Prikl. Spektrosk. 21 (1974) 357–359.

[19] U.K. Kang, A.A. Zhilin, D.P. Logvinov, et al., Transparent Nd^{3+}-activated glass-ceramics in the Li_2O–Al_2O_3–SiO_2 system: physicochemical aspects of their preparation and optical characteristics, Glass Phys. Chem. 27 (2001) 344–352.

[20] U.K. Kang, T.I. Chuvaeva, A.A. Onushchenko, et al., Radiative properties of Nd-doped transparent glass-ceramics in the lithium aluminosilicate system, J. Non-Cryst. Solids 278 (2000) 75–84.

[21] K.G. Cheng, Carbon effects on crystallization kinetics of Li_2O–Al_2O_3–SiO_2 glasses, J. Non-Cryst. Solids 238 (1998) 152–157.

[22] M. Avrami, Kinetics of phase change, J. Chem. Phys. 7 (1939) 1103–1112; 9 (1939) 177–184.

[23] W.A. Johnson, K.F. Mehl, Reaction kinetics in process of nucleation and growth, Trans. AIME 135 (1939) 416–442.

[24] H.E. Kissinger, Variation of peak temperature with heating rate in differential thermal analysis, J. Res. Natl. Bureau Standards 57 (1956) 217–221.

[25] J.A. Augis, J.E. Bennett, Calculation of the Avrami parameters for heterogeneous solid state reactions using a modification of the Kissinger method, J. Therm. Anal. 13 (1978) 283–292.